CHIN. PHYS. LETT. Vol. 36, No. 12 (2019) 124207

Identifying the Symmetry of an Object Based on Orbital Angular Momentum through a Few-Mode Fiber *

Zhou-Xiang Wang(王周祥)[1], Yu-Chen Xie(谢语晨)[1], Han Zhou(周寒)[1], Shuang-Yin Huang(黄双印)[1], Min Wang(王敏)[1], Rui Liu(刘瑞)[1], Wen-Rong Qi(齐文荣)[1], Qian-Qian Tian(田倩倩)[1], Ling-Jun Kong(孔令军)[2,3], Chenghou Tu(涂成厚)[1], Yongnan Li(李勇男)[1], Hui-Tian Wang(王慧田)[2,3]**

[1]*School of Physics and Key Laboratory of Weak-Light Nonlinear Photonics, Nankai University, Tianjin 300071*
[2]*School of Physics and National Laboratory of Solid State Microstructures, Nanjing University, Nanjing 210093*
[3]*Collaborative Innovation Center of Advanced Microstructures, Nanjing 210093*

(Received 29 October 2019)

In recent years, orbital angular momentum (OAM), as a new usable degree of freedom of photons, has been widely applied in both classical optics and quantum optics. For example, digital spiral imaging uses the OAM spectrum of the output beam from the object to restore the symmetry information of the object. However, the related experiments have been carried out in free space so far. Due to the poor anti-noise performance, limited transmission distance and other reasons, the practicability is seriously restricted. Here, we have carried out a digital spiral imaging experiment through a few-mode fiber, to achieve the identification of the symmetry of object by measuring the OAM spectrum of the output beam. In experiment, we have demonstrated the identification of the symmetry of amplitude-only and phase-only objects with the two-, three- and four-fold rotational symmetries. We also give the understanding of the physics. We believe that our work has greatly improved the practical application of digital spiral imaging in remote sensing.

PACS: 42.50.Tx, 42.30.Va, 42.81.−*i* DOI: 10.1088/0256-307X/36/12/124207

One of the many applications of optics is imaging to probe the structures of objects. A variety of imaging methods that use different degrees of freedom of light (e.g., intensity, wavelength, and polarization) have quickly developed. Until 1992, Allen *et al.* recognized that a helical (vortex) beam with an azimuthal phase of $\exp(jl\varphi)$ carries an orbital angular momentum (OAM) of $l\hbar$ per photon, where l is the topological charge (azimuthal mode index) and $\hbar$ is the reduced Plank constant.[1] The OAM eigenstates $|l\rangle$ form an infinite-dimensional orthogonal and complete basis.[2]

The discrete OAM spectrum (or spiral spectrum) is useful for imaging. When a beam illuminates an object, the OAM spectrum of the output beam can carry the symmetry information of the object, which is called digital spiral imaging.[3] This imaging technique can also be applied in many fields, such as probing the canonical geometric objects[4] and characterizing the location of dielectric particle on the micrometer scale.[5] In addition, digital spiral imaging experiments based on ghost imaging have been carried out. In 2012, Simon and Sergienko[6] presented two-photon spiral imaging with correlated OAM states, showing that the value of the mutual information depends strongly on object shape and is closely related to the degree of rotational symmetry. In 2013, using correlated photon pairs produced by spontaneous parametric down-conversion (SPDC), high-efficiency object identification was experimentally demonstrated based on the off-diagonal correlation effect in the OAM correlation matrix.[7] In 2014, quantum analogy of digital spiral imaging was achieved.[8] In 2017, identification of the spatial signatures and phase information of rotational-symmetry objects were demonstrated by classical OAM correlations in random light.[9] However, all the previous related works[3−9] were carried out in free space, which have some disadvantages as follows: (i) it is greatly affected by environmental instabilities, such as turbulence and impurity scattering in the air; (ii) it is difficult to bypass the obstacle; and (iii) it is hard to be tested in the narrow or curved space.

In recent years, some researchers have explored the transmission properties of OAM in fibers. In 2013, OAM multiplexing in specially designed fibers has been demonstrated without multiple-input multiple-output digital signal processing (MIMO-DSP).[10] In addition, the OAM multiplexing with large crosstalk in few-mode fibers (FMFs) has also been demonstrated by MIMO-DSP.[11,12] In our previous work, we studied the propagation property of OAM in commercial step-index FMFs.[13]

In this work, we carry out digital spiral imaging experiment to realize the symmetry recognition of the object after the probe beam passes through a commercial step-index FMF. The FMF we used is an OFS-1550TMF fiber, which is a two-mode fiber at 1550 nm, but more modes can be supported in the 810 nm we used here. The objects that we used, which are amplitude-only and phase-only, are constructed by hologram loaded on spatial light modulator (SLM). We also give a theoretical understanding. We synthe-

*Supported by the National Key R&D Program of China under Grant Nos 2017YFA0303800 and 2017YFA0303700, the National Natural Science Foundation of China under Grant Nos 11534006, 11674184, 11774183 and 11804187, the Natural Science Foundation of Tianjin under Grant No 16JCZDJC31300, and the Collaborative Innovation Center of Extreme Optics.
**Corresponding author. Email: htwang@nju.edu.cn
© 2019 Chinese Physical Society and IOP Publishing Ltd

size and measure the OAM spectrum and then to find the number of peaks in the OAM spectrum, finally to reveal the object symmetry. Our method can overcome the disadvantage of digital spiral imaging in free space, as mentioned above. Our method has greatly improved the practicality of identifying the symmetry of objects in remote sensing, by using OAM.

Linear momentum and linear position, angular momentum and angular position are also mutual Fourier transform pairs. The Fourier relation is associated with the Heisenberg uncertainty principle in quantum field.[14,15] For the azimuthal-varying function $\psi(\varphi)$, its Fourier transform and its inverse Fourier transform can be written as

$$A(l) = \frac{1}{2\pi}\int_{-\pi}^{\pi}\psi(\varphi)\exp(-jl\varphi)d\varphi, \tag{1a}$$

$$\psi(\varphi) = \sum_{l=-\infty}^{+\infty}A(l)\exp(jl\varphi). \tag{1b}$$

If a beam with a complex amplitude of $\psi(\varphi)$ is not azimuthal-variant, i.e. $\psi(\varphi) =$ constant, we have $A(l) = \delta(0)$ (where $\delta(x)$ is the well-known Dirac function), implying that such a beam carries no OAM. If the beam is confined in the azimuthal direction to become an amplitude-only sector beam with a sector angle of θ as

$$\psi(\varphi) = \begin{cases} 1 & \text{within } \varphi \in [-\theta/2, \theta/2], \\ 0 & \text{otherwise.} \end{cases} \tag{2}$$

From Eq. (1) we easily obtain its OAM spectrum to be $A(l) = (\theta/2\pi)\text{sinc}(l\theta/2)$. The OAM spectrum of the beam confined in the azimuthal direction is broadened symmetrically with respect to the strongest OAM component of $l\hbar = 0$, and all the OAM components are in-phase. If the beam with m-fold rotational symmetry is composed of m identical amplitude-only sector sub-beams (where m is a positive integer) as

$$\psi(\varphi) = \begin{cases} 1 & \text{within } \varphi \in \left[-\frac{\theta}{2}+\frac{2n\pi}{m}, \frac{\theta}{2}+\frac{2n\pi}{m}\right], \\ 0 & \text{otherwise,} \end{cases} \tag{3}$$

where $n \in [0, m-1]$ is a non-negative integer and indicates the order number of the sector. With Eq. (1), we easily obtain the OAM spectrum as

$$A(l) = \frac{m\theta}{2\pi}\text{sinc}\left(\frac{l\theta}{2}\right)\delta(l - Nm), \tag{4}$$

where N is an arbitrary integer. We find from Eq. (4) that due to the presence of the rotational symmetry, only the OAM components being the integer multiple of $m\hbar$ exist, while all other OAM components disappear. All the OAM components of $l\hbar = Nm\hbar$ are in-phase. Clearly, for the amplitude-only m-fold rotational symmetry beam, the OAM components of $l\hbar = \pm m\hbar$ are secondary-strongest except for the strongest OAM component of $l\hbar = 0$. If the beam is a phase-only m-fold rotational symmetry beam, as

$$\psi(\varphi) = \begin{cases} 1 & \text{within } \varphi \in \left[-\frac{\theta}{2}+\frac{2n\pi}{m}, \frac{\theta}{2}+\frac{2n\pi}{m}\right], \\ \exp(j\phi_0) & \text{otherwise.} \end{cases} \tag{5}$$

With Eq. (1), we easily obtain the OAM spectrum as

$$A(0) = \frac{m\theta}{2\pi} + \exp(j\phi_0)\left(1 - \frac{m\theta}{2\pi}\right), \tag{6a}$$

$$A(l) = [1 - \exp(j\phi_0)]\frac{m\theta}{2\pi}\text{sinc}\left(\frac{l\theta}{2}\right)\delta(l - Nm), \quad \text{for } l \neq 0. \tag{6b}$$

If the phase difference $\phi_0 = 0$, the m-fold phase-only beam described by Eq. (5) degenerates into the uniform beam, there has no OAM components except for $l\hbar = 0$ as shown above. If the phase difference $\phi_0 = \pi$, the OAM component of $l\hbar = 0$ is dramatically suppressed even disappear (when $\theta = \pi/m$); only the OAM components being the integer multiple of $m\hbar$ exist and are also in-phase, while all other OAM components disappear. Different from the amplitude-only m-fold rotational symmetry beam, the OAM components of $l\hbar = \pm m\hbar$ are strongest. For the general case ($\phi_0 \neq 0$ or $\phi_0 \neq \pi$), the OAM components of $l\hbar = \pm m\hbar$ are at least secondary-strongest except for the OAM component of $l\hbar = 0$. Therefore, such a special property of the OAM spectrum can be used to identify the rotational symmetry for both amplitude-only and phase-only beams (objects) in free space.

We now explore the identification of the symmetry of object by measuring the OAM spectrum of the output beam through an FMF. As we demonstrated,[13] during the transmission of the OAM mode in an FMF, its handedness is hard to be maintained completely, but its absolute value (i.e., topology of OAM mode) can be protected. Such a transmission characteristic of FMFs provides a possibility to recognize the symmetry of object when the beam carrying the symmetry information of object passes through an FMF.

When a beam passes through an object, the transmitted beam is coupled into an FMF, the output beam from the FMF should be $\psi_{\text{out}}(\varphi) = h_{\text{fiber}}(\varphi)h_{\text{obj}}(\varphi)\psi_{\text{in}}(\varphi)$, where $\psi_{\text{in}}(\varphi)$, $h_{\text{obj}}(\varphi)$, and $h_{\text{fiber}}(\varphi)$, being all azimuth-dependent, indicate the amplitude of the input beam, the transmission function of the object, and the transmission function of the FMF, respectively. Based on the convolution theorem of the Fourier transform, we have the following relation, $A_{\text{out}}(l) = H_{\text{fiber}}(l) \otimes H_{\text{obj}}(l) \otimes A_{\text{in}}(l)$, where $H_{\text{fiber}}(l) = \mathcal{F}\{h_{\text{fiber}}(\varphi)\}$ and $H_{\text{obj}}(l) = \mathcal{F}\{h_{\text{obj}}(\varphi)\}$ are impulse response functions of the FMF and the object, while $A_{\text{in}}(l) = \mathcal{F}\{\psi_{\text{in}}(\varphi)\}$ and $A_{\text{out}}(l) = \mathcal{F}\{\psi_{\text{out}}(\varphi)\}$ are the OAM spectra of the input and output beams, and $\mathcal{F}\{\}$ represents the Fourier transform operator, respectively.

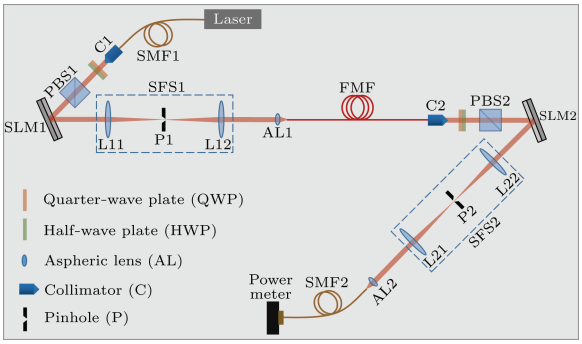

Fig. 1. Experimental setup. Laser: an fs laser at a central wavelength of 810 nm with a pulse duration of ∼140 fs and a repetition rate of 80 MHz. PBS: polarizing beam splitter; SLM: spatial light modulator; L11, L12, L21 and L22: lenses with the same focal length of 100 mm; SFS: spatial filtering system; SMF: single-mode fiber; FMF: few-mode fiber with a length of 150 m.

To explore the propagation properties of the OAM modes through an FMF, it is difficult to calculate theoretically the impulse response function (or the transmission function) of the FMF. It is more valid and practical that we use the experimental measurement instead of the theoretical calculation. When the input beam with no spatial structure [i.e. $\psi_{\rm in} \equiv 1$, with its OAM spectrum of $A_{\rm in}(l) = \delta(0)$] is coupled directly into an FMF without passing through the object, the measured OAM spectrum $A_{\rm out}(l)$ of the output beam from the FMF represents in fact the impulse response function of the FMF [i.e. $H_{\rm fiber}(l) = A_{\rm out}(l)|_{\psi_{\rm in}\equiv 1 \cap h_{\rm obj}(\varphi)\equiv 1}$]. When we want to explore the symmetry of the object using the digital spiral imaging through an FMF, the beam illuminating the object should select to be no spatial structure. Therefore, when an m-fold rotational symmetry object is inserted into the optical path, the OAM spectrum of the output beam from the FMF should be $A_{\rm out}(l) = H_{\rm fiber}(l) \otimes H_{\rm obj}(l)$.

We now demonstrate our idea experimentally. The experimental setup is shown in Fig. 1, in which the light source is a femtosecond (fs) laser at a central wavelength of 810 nm with a pulse duration of ∼140 fs and a repetition rate of 80 MHz. The fs laser beam is coupled into SMF1 to perform the spatial filtering and to preserve the fundamental Gaussian mode. The output beam from SMF1 is collimated by C1, and then its polarization state is controlled by the first set of QWP, HWP and PBS1 to be horizontally polarized, due to the requirement of SLM1. The hologram loaded on SLM is used to produced the object. On the one hand, it is easy to make the comparison without re-collimating the optical path in the same circumstance; on the other hand, it is easy to simulate any desired structures of amplitude-only or phase-only objects. In our experiment, although the SLM we used is phase-only, the blazed holographic grating loaded on the SLM1 can also modulate the amplitude. The first-order diffraction from the hologram loaded on the SLM1 is extracted by SFS1 (containing P1 and a $4f$ system composed of L11 and L12). AL1 with a focal length of 11 mm couples the beam carrying the object information into a 150-m-long FMF (OFS-1550TMF). The output beam from the FMF is collimated by C2. The second set of QWP, HWP and PBS2 controls the beam incident on the SLM2 to be horizontally polarized. We now need the projection measurement for the OAM spectrum of the output beam from the FMF, by using the forked gratings (loaded on SLM2) with different topological charges in turn. The OAM component (we want to measure) of the output beam from the FMF can be converted by the forked grating with a suitable topological charge into the fundamental Gaussian mode, which is the first-order diffraction from SLM2. It is extracted and filtered by SFS2 (containing P2 and another $4f$ system composed of L21 and L22). The extracted fundamental Gaussian mode is coupled by AL2 into SMF2 and then is detected by the power meter.

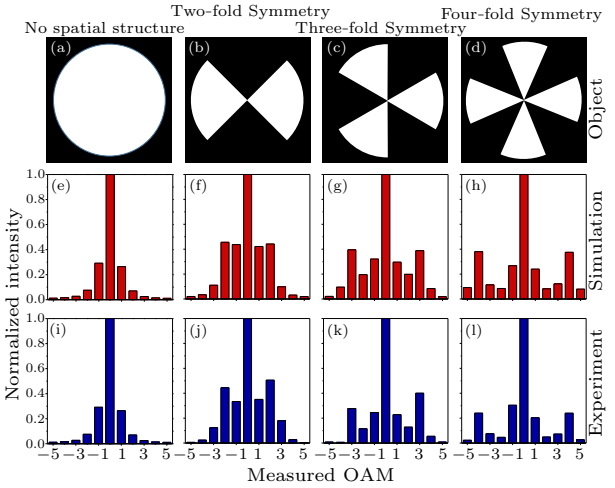

Fig. 2. OAM spectra of the beams passing through the amplitude-only rotational symmetric objects and FMF. The first row shows the amplitude-only objects, where only the white sectors allow the light to be passed through. Correspondingly, the second and third rows show the simulated and measured OAM spectra of the outputs from the FMF, respectively. The first, second, third and fourth columns correspond to the objects of no spatial structure, two-fold, three-fold and four-fold symmetries, respectively.

We first explore the projection measurement of OAM spectra after the beam passing through an amplitude-only rotational symmetric object and an FMF in turn. As shown in the first row of Fig. 2, the amplitude-only objects produced by the holograms loaded on SLM1, from left to right, correspond to the objects of no spatial structure, two-fold, three-fold and four-fold symmetries, respectively. The second and third rows in Fig. 2 show the simulated and measured OAM spectra, respectively. One should point out that, as mentioned above, we use the measured impulse response function of the FMF for simulation. One can see that when the object has no spatial structure, the output OAM spectrum from the FMF exhibits an approximate Gaussian distribution, in which the component of OAM = 0 is strongest. However, both the simulated and measured results demonstrate that for the two-fold (three-fold) symmetric object, the components of OAM = ±2 (OAM = ±3) are sig-

nificantly enhanced and are the secondary-strongest ones except for the component of OAM = 0. For the four-fold symmetric object, the simulated result shows that the components of OAM = ±4 are also significantly enhanced and are the secondary-strongest ones; but the measured result shows that the component of OAM = −1 is stronger than the components of OAM = ±4. Therefore, for the amplitude-only object with $\theta = \pi/m$, we can on the whole identify the rotational symmetry of an object from the measured OAM spectrum, but we cannot completely identify it.

Next, we would like to explore the phenomena when the beam passes through a phase-only rotational symmetric object and an FMF in turn. As shown in Fig. 3, the first row depicts the phase-only objects produced by the holograms loaded on SLM1, from left to right, correspond to the objects with no spatial structure, two-, three- and four-fold symmetries, respectively. The second (third) row in Fig. 3 shows the simulated (measured) results of OAM spectra of the output from the FMF. We find that the experimentally observed results are in good agreement with the simulated results. Firstly, for an m-fold symmetry phase-only object, in the OAM spectra of the output beam from the FMF, the OAM = $\pm m$ components are greatly enhanced as the amplitude-only cases. However, the phase-only cases have significant differences from the amplitude-only cases: (i) The OAM = $\pm m$ components are the strongest ones. (ii) The OAM = 0 component is the weakest one even to be zero. As a result, for the phase-only object with $\theta = \pi/m$, we can completely identify the rotational symmetry of an object from the measured OAM spectrum.

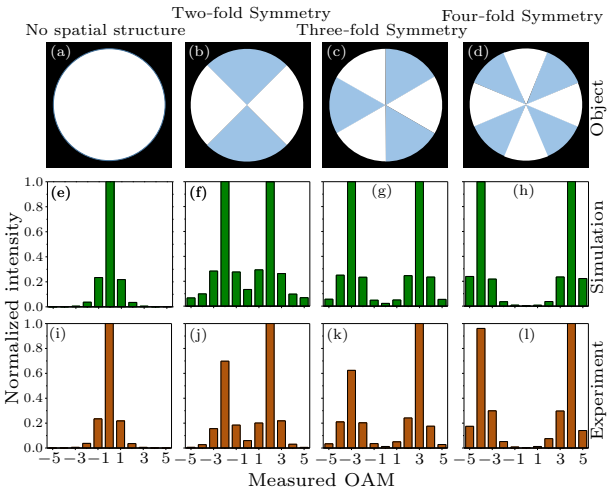

Fig. 3. OAM spectra of the beams passing through the phase-only rotational symmetric objects and the FMF. The first row shows the phase-only objects, where there is a phase difference of π between the pale blue sectors and the white sectors. Correspondingly, the second and third rows show the simulated and measured OAM spectra of the outputs from the FMF, respectively. The first, second, third and fourth columns correspond to the objects of no spatial structure, two-fold, three-fold and four-fold symmetries, respectively.

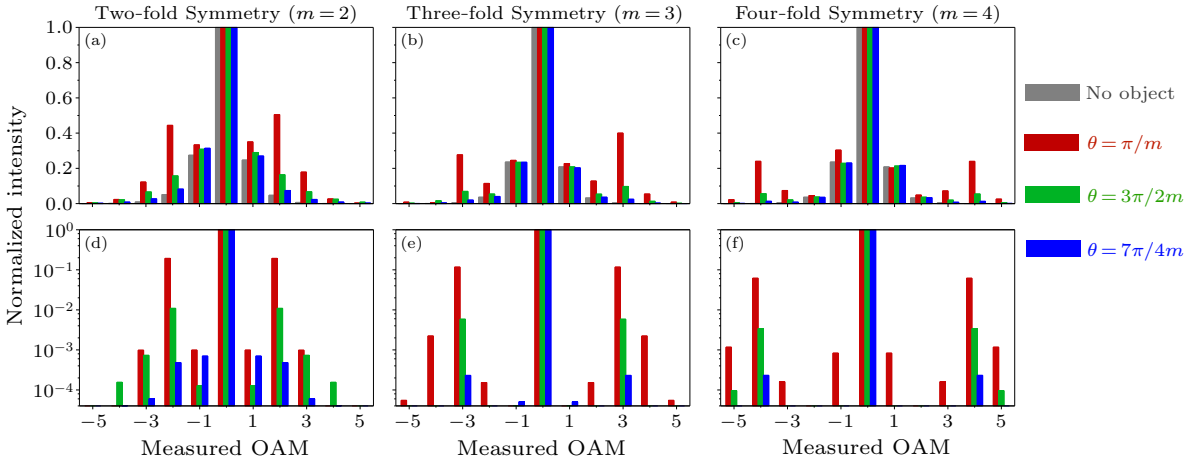

Fig. 4. Dependence of the OAM spectrum on the sector angle θ for amplitude-only objects with different rotational symmetries. (a)–(c) The measured OAM spectra of the output beams from the FMF, for the three objects with the two-, three- and four-fold symmetries, respectively, in which the gray bar graph is the OAM spectrum with no object and indicates in fact the impulse response function of the FMF. (d)–(f) The deconvolution results of the OAM spectra, corresponding to (a)–(c), respectively.

One should note that we focused only on the situations of $\theta = \pi/m$ in the above that all the sectors have the same sector angle in Figs. 2 and 3. We will explore the influence of the different sector angle θ. The dependence of the measured OAM spectrum on the sector angle θ for three different amplitude-only objects with the two-, three- and four-fold rotational symmetries are shown in Figs. 4(a)–(c), respectively, where the gray bar graph indicates the impulse response function of the FMF. Except for the case of $\theta = \pi/m$, it is hard to directly identify the rotational symmetry of the object from the measured OAM spectrum of the output beam from FMF. The dominant reason is the broadening of OAM spectrum caused by the FMF. A solution is to perform the deconvolution to eliminate the influence of the FMF, because $A_{\text{out}}(l) = H_{\text{fiber}}(l) \otimes H_{\text{obj}}(l)$ as shown above. We need to perform the inverse Fourier transforms, $\mathcal{F}^{-1}\{H_{\text{fiber}}(l)\}$ and $\mathcal{F}^{-1}\{A_{\text{out}}(l)\}$. Finally, we can obtain the OAM spectrum of the object,

as $H_{\rm obj}(l) = \mathcal{F}\{\mathcal{F}^{-1}\{A_{\rm out}(l)\}/\mathcal{F}^{-1}\{H_{\rm fiber}(l)\}\}$. The deconvolution results of the OAM spectra shown in Figs. 4(d)–(f) reveal the fact that the OAM spectrum can identify the rotational symmetry of an amplitude-only object, that is to say, the strongest OAM components except for $l\hbar = 0$ are $l\hbar = \pm m\hbar$. However, there is an exception that for the case of $m = 2$ and $\theta = 7\pi/4m$, the OAM components of $l\hbar = \pm 2\hbar$ are slightly weaker than those of $l\hbar = \pm\hbar$, which may be caused by measurement error.

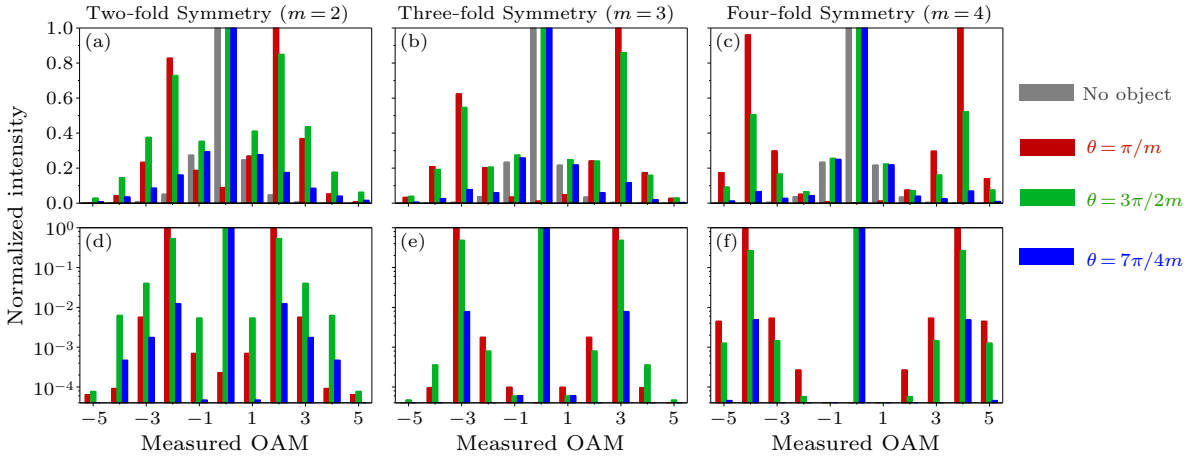

Fig. 5. Dependence of the OAM spectrum on the sector angle θ for phase-only objects ($\phi_0 = \pi$) with different rotational symmetries. (a)–(c) The measured OAM spectra of the output beams from FMF, for the three objects with the two-, three- and four-fold symmetries, respectively; in which the gray bar graph is the OAM spectrum with no object and indicates in fact the impulse response function of FMF. (d)–(f) The deconvolution results of the OAM spectra, corresponding to (a)–(c), respectively.

The dependence of the measured OAM spectrum on the sector angle θ for three different phase-only objects with the two-fold, three-fold and four-fold rotational symmetries are shown in Figs. 5(a)–5(c), respectively, where the gray bar graph still indicates the impulse response function of the FMF. Except for the case of $\theta = \pi/m$, it is also hard to directly identify the rotational symmetry of the object from the measured OAM spectrum of the output beam from the FMF. We also need again to perform the inverse Fourier transforms on the measured OAM spectra of the output beams from the FMF, passing and no passing through the objects, i.e. $\mathcal{F}^{-1}\{H_{\rm fiber}(l)\}$ and $\mathcal{F}^{-1}\{A_{\rm out}(l)\}$. The deconvolution results of the OAM spectra shown in Figs. 5(d)–5(f), $H_{\rm obj}(l) = \mathcal{F}\{\mathcal{F}^{-1}\{A_{\rm out}(l)\}/\mathcal{F}^{-1}\{H_{\rm fiber}(l)\}\}$, reveal the fact that the OAM spectrum can also identify the rotational symmetry of a phase-only object, that is to say, the strongest OAM components except for $l\hbar = 0$ are $l\hbar = \pm m\hbar$.

In discussion, the following points need to be stated. (i) As long as an object/beam has m-fold rotational symmetry, for any shape (sector, bar and so on), it can be decomposed into a series of OAM components, and the OAM components of $l\hbar = \pm m\hbar$ are strongest except for the OAM component of $l\hbar = 0$. Therefore, the regular angular distribution of the object (hologram) in this work is theoretically universal. (ii) After the experiment in this work was finished, we used the actual objects (bar-like objects) instead of the SLM1 to verify our results. The results are consistent with those in this work, which proves the universality of the conclusion. (iii) We use the prepared single photon source to replace the femtosecond laser in the present experiment, and obtain the same results. Because the uncertainty relation in quantum mechanics also satisfies Fourier transform, the conclusion in this work can also be applied to single photon level.

In summary, we have carried out digital spiral imaging experiment to realize the symmetry recognition of the object after the probe beam passing through a commercial step-index FMF. Our method can overcome the disadvantage of digital spiral imaging in free space. In addition, our method has greatly improved the practicality of digital spiral imaging for identifying the symmetry of objects in remote sensing by using OAM.

References

[1] Allen L et al 1992 *Phys. Rev. A* **45** 8185
[2] Molina-Terriza G et al 2001 *Phys. Rev. Lett.* **88** 013601
[3] Torner L et al 2005 *Opt. Express* **13** 873
[4] Molina-Terriza G et al 2007 *J. Eur. Opt. Soc.* **2** 07014
[5] Petrov D et al 2012 *Opt. Lett.* **37** 869
[6] Simon D S and Sergienko A V 2012 *Phys. Rev. A* **85** 043825
[7] Uribe-Patarroyo N et al 2013 *Phys. Rev. Lett.* **110** 043601
[8] Chen L et al 2014 *Light: Sci. & Appl.* **3** e153
[9] Yang Z et al 2017 *Light: Sci. & Appl.* **6** e17013
[10] Bozinovic N et al 2013 *Science* **340** 1545
[11] Wang J et al 2012 *Nat. Photon.* **6** 488
[12] Huang H et al 2015 *Sci. Rep.* **5** 14931
[13] Wang Z X et al 2019 *Chin. Opt. Lett.* **17** 120601
[14] Yao E et al 2006 *Opt. Express* **14** 9071
[15] Jack B et al 2008 *New J. Phys.* **10** 103013